Plant Soil
https://doi.org/10.1007/s11104-018-3692-8

REGULAR ARTICLE

Modification of plant cell wall chemistry impacts metabolome and microbiome composition in *Populus PdKOR1* RNAi plants

Allison M. Veach · Daniel Yip · Nancy L. Engle · Zamin K. Yang · Amber Bible · Jennifer Morrell-Falvey · Timothy J. Tschaplinski · Udaya C. Kalluri · Christopher W. Schadt

Received: 10 October 2017 / Accepted: 18 May 2018

Abstract
Aims We examined the effect of downregulating *PdKOR1* gene, an endo-β-1,4-glucanase gene family member previously characterized to affect cellulose biosynthesis and cell wall composition in *Populus*, on the secondary metabolome and microbiome of field-grown *Populus deltoides*.
Methods We revealed differences in metabolite profiles of *PdKOR1* RNAi and control roots using gas chromatography-mass spectrometry, and microbiome identification via Illumina MiSeq 16S and ITS2 rRNA sequencing in root endospheres and rhizospheres.
Results PdKOR1 RNAi root metabolites differed from control plants: free amino acids (valine, isoleucine, alanine) were reduced while caffeoyl-shikimates, salicylic-acid derivatives, and flavonoid metabolites increased in *PdKOR1* RNAi roots. The Actinobacterial family *Micromonosporaceae* were more abundant in RNAi root endospheres, whereas *Nitrospirae* was reduced in *PdKOR1* RNAi rhizospheres. *Ascomycota* were lower and *Basidiomycota* greater in *PdKOR1* rhizospheres. Bacterial and fungal community composition, as measured by Bray-Curtis dissimilarity, differed between *PdKOR1* RNAi and control rhizospheres and endospheres.
Conclusions These results indicate that modification of plant cell walls via downregulation of *PdKOR1* gene in *Populus* impacts carbon metabolism in roots and concomitant alterations in root-associated microbial communities. Such an understanding of functional and ecological implications of biomass chemistry improvement efforts is critical to address the goals of sustainable bioenergy crop production and management.

Keywords Cellulose · Cell wall alteration · Endo-1,4-ß-glucanase · Microbiome · Metabolome · *Populus*

Responsible Editor: Birgit Mitter.

Electronic supplementary material The online version of this article (https://doi.org/10.1007/s11104-018-3692-8) contains supplementary material, which is available to authorized users.

A. M. Veach · D. Yip · N. L. Engle · Z. K. Yang · A. Bible · J. Morrell-Falvey · T. J. Tschaplinski · U. C. Kalluri (✉) · C. W. Schadt (✉)
Biosciences Division, Oak Ridge National Laboratory, 1 Bethel Valley Road, Oak Ridge, TN 37831, USA
e-mail: kalluriudayc@ornl.gov; e-mail: schadtcw@ornl.gov

Introduction

Cellulose synthesis and cell wall formation are important processes which regulate plant structure and function. Differences in cell wall composition results in physiological changes, such as altered stress responses (Zhao and Dixon 2014), water transport (Liang et al. 2010), and growth rates (Thomas et al. 2013). As a consequence, cell wall structure strongly regulates plant development and overall health. Optimization of plant cell wall and lignocellulosic biomass composition, via

Published online: 04 June 2018

genetic modification or selection of cell wall pathway or carbon metabolism genes, are broadly-used strategies in advanced bioenergy feedstock improvement efforts (Fu et al. 2011; Kalluri et al. 2014; Li et al. 2016; Loqué et al. 2015; Petersen et al. 2012; Yang et al. 2013). Such strategies have been demonstrated to achieve shifts in lignin composition (Baxter and Stewart Jr 2013; Furtado et al. 2014), cellulose and hemicellulose content (Hernández-Blanco et al. 2007; Kalluri et al. 2016), and greater hexose:pentose ratios within wood tissue (Loqué et al. 2015) with the specific target of improving saccharification of lignocellulosic biomass. For the long-range goal of sustainable production of bioenergy crops, research efforts must co-optimize plants for biomass amount and composition as well as sustainable field performance characteristics such as enhanced water and nutrient-use efficiency, resistance to microbial pathogens, and interactions with beneficial microbes.

KORRIGAN (KOR) is a membrane bound endo-ß-1,4-glucanase (EGase) in the glycosyl hydrolase family 9 (GH9) (Urbanowicz et al. 2007; Vain et al. 2014) shown to be associated with the cellulose synthase complex (Darley et al. 2001; Joshi and Mansfield 2007). Previous characterization of KOR homologs in *Populus deltoides* has shown that RNAi-mediated downregulation of *KOR* (*PdKOR1* and *PdKOR2*) impacts an array of plant properties, including reductions in cellulose, lignin and soluble sugar content, increase in cellulose crystallinity and phenolic conjugates, and reduced stem and root growth (Bali et al. 2016; Kalluri et al. 2016). The altered carbon allocation and secondary metabolome of *PdKOR1* RNAi plants has been previously shown to increase colonization rates of the ectomycorrhizal fungal symbiont, *Laccaria bicolor* under greenhouse conditions (Kalluri et al. 2016). A broader understanding of plant – microbe interactions under field conditions and potential impacts on beneficial root endophytic and rhizospheric bacteria and fungi, in the context of modifying cellulose biosynthesis and secondary metabolism, is relatively unexplored.

Microbial establishment with plant hosts can confer benefits, such as antagonistic suppression of pathogens, enhanced nutrient acquisition, enhanced growth, and/or increased stress resiliency (Mendes et al. 2013) and plant hosts may also select for specific groups of beneficial microorganisms. For example, it has been reported that plants growing in contaminated soils show a preferential colonization by root endophytic microbes carrying toxin degradation genes (Siciliano et al. 2001; Thijs et al. 2016). Downregulation of a lignin biosynthesis gene and higher levels of phenolic metabolites in field-grown *Populus tremula x Populus alba* was also shown to alter bacterial community structure and metabolic capabilities in root endospheres via selection of the metabolically diverse *Pseudomonas putida* (Beckers et al. 2016). That study (Beckers et al. 2016) provided a novel insight that regulation of an enzyme integral for lignin production can have direct (i.e., modified lignin content and metabolite production) as well as indirect (i.e., large changes in overall plant phenotype) implications for host selection of microbial partners of transgenic tree species. Previous work also indicated *PdKOR1* RNAi plants have cascading effects on multiple phenotypic traits in *Populus* (Kalluri et al. 2016; Maloney and Mansfield 2010) resulting in significant impacts on interactions with a fungal mutualist (Kalluri et al. 2016).

Within this context, here we studied the impact of *PdKOR1* gene downregulation on the root secondary metabolome and the overall bacterial and fungal microbiomes within the rhizosphere and root endospheres in field-grown *Populus deltoides*. Our goals were to first examine how *PdKOR1* RNAi plants differed in secondary metabolites within field-grown root tissue and determine if such genotype-specific differences were associated with changes to root and rhizosphere microbiomes in field-grown *PdKOR1* RNAi plants. To further our understanding of bacteria community assembly within *Populus* downregulated in *PdKOR1*, we also examined the colonization patterns of a Gammaproteobacterium, *Pantoea* sp. YR343, a robust root colonizer of *Populus deltoides* (Bible et al. 2016; Estenson et al. 2018), in vector controls and RNAi transgenic plants grown in greenhouse settings.

Materials and methods

Transgenic plant generation and tissue collection

The methods used to generate *PdKOR* RNAi lines, and their growth and cell wall phenotypes have been previously described elsewhere in detail (Kalluri et al. 2016).

Briefly, a ~ 200-bp fragment was amplified from 3' UTR region of the *PdKOR1* gene, which contained partial homology to *PdKOR2* gene in *P. deltoides,* and was cloned into vector pAGSM552 and expressed under the control of an Ubiquitin promoter and transformed into *P. deltoides* 'WV94' for RNAi knockdowns. Clonal replicates of the transformants were grown in the greenhouse as well as maintained at a USDA permitted stoolbed site in Bellville, GA, USA for further study. Fine roots were harvested from three independent ramets (replicate plants) both from a *PdKOR1* RNAi and an empty vector control line in November 2016 by carefully tracing structural roots connected to the main stem. Root tissue and adhering rhizosphere soil was frozen immediately on dry ice and transported to Oak Ridge National Laboratory where they were stored at −80 °C until processing. Fine roots were separated from each sample and subsampled for microbiome and metabolome analyses. For microbiome analyses, roots were washed with sterile water, centrifuged to collect the rhizosphere soil fraction, and then surface sterilized as described previously in preparation for the extraction of root endosphere DNA (Shakya et al. 2013).

Metabolomic profiling

Root tissue metabolites were analyzed by using gas chromatography (GC)-mass spectrometry (MS). Approximately 170–200 mg of fine root tissue were extracted twice in 2.5 ml of 80% ethanol and 1 ml of extract was dried in liquid nitrogen. Sorbitol was added and also used as an internal standard for metabolite identification. Once an aliquot of the extract was dried, it was dissolved in acetonitrile, followed by trimethylsilylation (TMS), and analyzed on a GC-MS after 2 days, as described elsewhere (Payyavula et al. 2014). Metabolites were identified using the Wiley Registry 10th Edition with NIST 2014 mass spectral database and a large, user-created database (>2400 spectra) of 70 eV electron impact (EI) fragmentation patterns of TMS-derivatized metabolites.

DNA extraction and 16S and ITS2 library preparation

Separate 50-mg samples of surfaced sterilized root tissue (root endosphere) were frozen in liquid nitrogen and bead-beaten for 1 min with a sterile, 5-mm steel bead prior to extraction (Qiagen, Venlo, the Netherlands). This was repeated three times with samples placed in liquid nitrogen for 1 min between each bead-beating. DNA was then extracted using the MoBio PowerPlant Pro DNA Isolation Kit (MoBio Laboratories, Inc., Carlsbad, CA, USA) and quantified on a NanoDrop 1000 spectrophotometer (NanoDrop Products, Wilmington, DE, USA). Genomic DNA was then purified and concentrated using a Zymo DNA Clean and Concentrator – 5 Kit (Zymo Research Corporation, Irvine, CA, USA) and quantified again prior to PCRs. Rhizosphere soil samples had DNA extracted using the MoBio PowerSoil DNA Isolation Kit (MoBio Laboratories, Inc., Carlsband, CA, USA) using standard procedures and similarly quantified prior to PCRs.

A two-step PCR approach was used with frameshifting nucleotide primers (Lundberg et al. 2013) with the following modifications. Primary PCRs consisted of forward and reverse primer mixtures modified to maximize phylogenetic coverage of archaea, bacteria, and fungi (Online Resource 1). Primers for bacterial and archaeal amplicons included a mixture of 8 forward 515F and 6 reverse 806R primers. Specifically, 515F universal primers (87%), Archaea (10%), and TM7 (3%) forward primers targeted at the V4 gene region of the 16S rRNA gene were supplied in PCRs. Primers for fungal amplicons included a mixture of 11 forward and 6 reverse primers at equal concentration (0.5 μM). In addition, a peptide nucleotide acid (PNA) blocker oligos (PNA Bio Inc., Thousand Oaks, CA, USA) targeted at plant mitochondrial and plastid 16S rRNA genes and the plant 5.8S nuclear rRNA gene upstream of ITS2 gene region was included in PCRs (Online Resource 1). The mitochondrial PNA was similar to Lundberg et al. 2013, except adjusted for a 1 bp mismatch in *Populus* spp. The 5.8S PNA was custom designed for *Populus*-fungal amplicon studies as described previously (Cregger et al. 2018). Primary PCR thermal cycler conditions for rhizospheres were 5 cycles of 95 °C for 1 min., 50 °C for 2 min., and 72 °C for 1 min. PCR conditions for root endospheres were 5 cycles of 95 °C for 1 min., 78 °C for 5 s., 50 °C for 2 min., and 72 °C for 1 min. Primary PCR products were then cleaned with Agencourt AMPure beads at a 0.7 to 1 ratio. Secondary PCRs included cleaned PCR products as the DNA template (20 ul from 21 ul of cleaned product), and barcoded reverse primers and forward primers in 50 ul reactions. Thermal cycler conditions for rhizosphere secondary PCRs were 95 °C for 45 s., followed by 32 cycles of 95 °C for 15 s., 60 °C for 30 s.,

72 °C for 30 s., and final extension at 72 °C for 30 s. Secondary PCR conditions for endospheres included 95 °C for 45 s., followed by 32 cycles of 95 °C for 15 s., 78 °C for 5 s., and all other parameters the same as rhizosphere secondary PCRs. After secondary DNA-tagging PCRs were completed, samples were pooled based on band intensity (agarose gel, 1.2% *w/v*) and purified with Agencourt AMPure XP beads (0.7 to 1 ratio; Beckman Coulter Inc., Pasadena, CA, USA). Both 16S and ITS2 libraries were sequenced using Illumina MiSeq (v. 2, 2 × 250 cycles) with a 9 pM amplicon concentration and a 15% PhiX spike.

Bioinformatics analysis

Paired-end sequences (.fastq) had primers removed on each .fastq individually using the cut adapt program (Martin 2011). All other analyses were performed in QIIME (Caporaso et al. 2010). Sequences were then joined and demultiplexed with a Phred quality threshold of 20. After demultiplexing, there were 1,886,726 sequences for 16S and 325,442 sequences for ITS2 libraries. Chimeras were detected using the UCHIME algorithm (Edgar et al. 2011), filtered and resulting sequences had operational taxonomic units (OTUs) clustered at a 97% sequence similarity using the open reference workflow and the SILVA database (release 128; Quast et al. 2013) for archaea and bacteria and the UNITE database (Abarenkov et al. 2010) for fungi with singleton OTUs removed prior to clustering. After these steps, there were 1,849,222 sequences for 16S rRNA and 323,770 sequences for ITS2. Representative sequences for successfully aligned OTUs for 16S rRNA were classified using the RDP Naïve Bayesian Classifier (Wang et al. 2007) whereas unaligned ITS2 sequences were classified using BLAST implemented via QIIME. OTUs unclassified at the domain level, mitochondrial, and chloroplast sequence contaminants were identified and removed for bacteria (1,532,220 sequences retained) whereas any unclassified OTUs at kingdom level or contaminants from plants or protists were filtered for fungi (315,709 sequences retained). Samples were rarefied at 30,000 sequences per sample for bacteria and 8000 per sample for fungi. The final bacterial dataset had 13,858 OTUs and 300,000 sequences whereas the fungal dataset has 1453 OTUs and 80,000 sequences. Microbial diversity metrics were estimated from the rarefied dataset via QIIME and included observed OTU richness, Simpson's Diversity, Simpson's Evenness, and Faith's Phylogenetic Diversity, the latter (Faith's PD) for archaea and bacteria only. Sequence data is archived through NCBI Sequence Read Archive under BioProject Accession PRJNA400443 (16S) and PRJNA433541 (ITS2).

Pantoea inoculation experiment

We used *Pantoea* sp. YR343 as inoculation in greenhouse co-culture experiments as it is a known root colonizer, which has been well characterized in previous works with wild type *Populus* (Bible et al. 2016; Estenson et al. 2018). *Pantoea* sp. YR343 was used to examine how *PdKOR1* downregulation affects colonization in the rhizosphere under controlled, greenhouse conditions as a previous GFP modification made microscopic examination and quantification possible. Greenwood cuttings of *Populus deltoides* vector control and the *PdKOR1* RNAi transgenic lines were rooted and grown in the greenhouse in leach tubes containing Fafard Professional Potting Mix soil (Sun Gro Horticulture, Agawam, MA, USA) for 3 months in the spring of 2017. The plants were transplanted to bigger pots (ShortOne Tree Pots; Steuwe & Sons, Inc., Tangent, Oregon, USA) containing autoclaved sterile soil preceding the introduction of microbial inoculum. Wild-type *Pantoea* YR343 chromosomally tagged with Green Fluorescent Protein (GFP) (YR343-GFP; with gentamycin selection marker) (Bible et al. 2016) were grown overnight in R2A liquid media, washed in PBS, then the OD_{600} was adjusted to 0.1 for a total volume of 2 ml approximately equivalent to 10^7 cells. Control plants were treated with 2 ml of sterile PBS and experimental plants were treated with 2 ml of bacterial culture. Irrigation was continued the following day. Three weeks post-inoculation, plants were harvested, and root tissue was washed with water to remove excess soil. A portion of root tissue for each plant was then measured and washed with PBS and glass beads, as described previously (Bible et al. 2016). The wash was then serially diluted and plated on R2A agar containing 10 μg ml^{-1} gentamycin in order to select for YR343-GFP. Colony forming units (CFUs) were counted and standardized by total root weight. Sections of root sample were also used for imaging analysis using a Zeiss LSM 710 confocal microscope (Zeiss, Oberkochen, Germany). Imaging was performed by placing small root sections on a glass slide with water and imaged with the following excitation parameters: 488 nm for

green fluorescence of *Pantoea* YR343-GFP, and 561 nm for red autofluorescence of plant tissue.

Statistical analysis

Four replicates for both root endosphere and rhizospheres were originally included for RNAi plant samples. Unfortunately, fine roots were limited and metabolomic analyses required all fine-root tissue for 2 of 4 *PdKOR1* RNAi samples, therefore only 2 replicates are given for microbial community results ($n = 2$ for RNAi plants). A Student's t-test was performed to determine if individual metabolites and *Pantoea* colonization, as determined by CFUs, differed between *PdKOR1* RNAi and control plants. Furthermore, we calculated the relative abundances of dominant taxa (≥1% relative abundance; families, phyla or subphyla for Proteobacteria and at the order and phyla levels for fungi) and diversity estimates and compared between *PdKOR1* RNAi and vector control tissues using Welch's two-sample t-tests. We chose to target fungal orders instead of families as many fungal OTUs were not classified to the family level (63% unclassified to family). For microbial community composition, Bray-Curtis dissimilarity was calculated and used as input for principal coordinates analysis (PCoA). An adonis analysis, similar to a permutational multivariate ANOVA (perMANOVA; permutations = 999), was then used with Bray-Curtis as input to detect if habitat (rhizosphere versus endosphere) or transgenic line (*PdKOR1* RNAi versus control) significantly explained variation in microbial community composition. All analyses were performed in R (version 3.3.2; R Core Team 2016) using the stats (*t.test* function), labdsv (*pco* function; Roberts 2016), and vegan (*adonis* function; Oksanen et al. 2017) packages.

Results

Metabolomic profiling

There were 171 distinct metabolites detected in fine root tissues (Online Resource 2). Among these metabolites, 54 (31%) were differentially abundant between *PdKOR1* RNAi plant and control plant roots ($p \leq 0.05$; Table 1). Several of these were caffeic acid derivatives, which included caffeoyl conjugates, caffeoyl glycoside conjugates, and caffeoyl shikimate conjugates (Table 1). Interestingly, certain derivatives were not detectable in *PdKOR1* RNAi tissues while present in controls. Caffeic acid derivatives, notably caffeoyl shikimate conjugates, were upregulated in RNAi tissue and were at very low concentrations in control root tissue (Table 1). Furthermore, palmitic acid and docosanoic acid, involved in fatty acid metabolism, and salicylic acid-related metabolites, such as salicyl alcohol (1.77 fold increase) and isosalicin (3.62 fold increase), were produced in greater concentrations in *PdKOR1* RNAi roots ($p \leq 0.04$). Flavonoid metabolites were also produced higher in *PdKOR1* RNAi root tissue and had approximately 4–5-fold increases (Table 1) whereas a guaiacyl lignan metabolite (16.55297225 lignan) was also greater (2.8-fold increase) in *PdKOR1* RNAi plant roots (Table 1). Conversely, amino acids including valine, isoleucine, threonine, alanine, and serine, were reduced in *PdKOR1* RNAi plants relative to control plants ($p \leq 0.01$; Table 1).

Microbial diversity and community structure

Rhizospheres had greater bacterial (13% greater) and fungal diversity (45% greater) than root endospheres (Table 2). Rhizosphere communities were dominated by *Alphaproteobacteria*, *Actinobacteria*, and *Acidobacteria* primarily (Fig. 1), whereas root endosphere communities were dominated by *Actinobacteria*, *Alphaproteobacteria*, and *Gammaproteobacteria* (Fig. 1). Rhizosphere microbial communities from controls had, on average (± s.e.), greater abundances of *Nitrospirae* (2 ± 0.2%) compared to *PdKOR1* RNAi plants (0.7 ± 0.1%, $T = -4.87$, $p = 0.02$; Fig. 1). Furthermore, the *Ascomycota* ($T = -4.73$, $p = 0.03$) and *Basidiomycota* ($T = 6.85$, $p = 0.01$) fungal phyla differed in relative abundance between *PdKOR1* RNAi and control rhizospheres. *PdKOR1* rhizospheres were significantly lower in *Ascomycota* (35 ± 4% versus 61 ± 4%) and greater in *Basidiomycota* (58 ± 3% versus 29 ± 3%) compared to controls (Fig. 1). Interestingly, our previous co-culture study using a known mycorrhizal basidiomycete species, *Laccaria bicolor*, showed higher root colonization rates with *PdKOR1* RNAi plants relative to control plants (Kalluri et al. 2016). Overall, we observed phyla-level differences among

Table 1 Summary statistics (mean ± standard error) for differentially produced root metabolites among *PdKOR1* RNAi and vector control roots ($p < 0.05$, Student's t-test)

Metabolite	*PdKOR1* (μg/g FW)	Control (μg/g FW)	Fold change – *PdKOR1*
24.21271219289582567 caffeoyl conjugate	0	37.9 ± 3.8	0
21.70171 caffeoyl glycoside conjugate	0	78.6 ± 15.2	0
21.24171 caffeoyl glycoside conjugate	0	101.0 ± 23.9	0
16.13328 glycoside	9.7 ± 1.7	50.4 ± 4.8	0.19
phosphate	494.7 ± 148.3	1389.6 ± 72.7	0.36
serine	33.0 ± 4.6	84.2 ± 2.3	0.39
alanine	54.2 ± 9.3	135.9 ± 8.3	0.40
threonine	7.6 ± 1.0	18.9 ± 0.9	0.40
16.67 syringl lignan	6.4 ± 0.8	13.9 ± 0.8	0.46
isoleucine	3.7 ± 0.4	7.8 ± 0.9	0.48
valine	10.0 ± 1.1	19.9 ± 1.4	0.50
a-linolenic acid	17.0 ± 0.7	12.7 ± 0.7	1.34
linoleic acid	22.5 ± 1.6	16.8 ± 0.5	1.34
glycerol	19.5 ± 1.0	14.1 ± 1.6	1.39
stearic acid	7.6 ± 0.5	5.2 ± 0.4	1.45
pinoresinol	2.5 ± 0.2	1.6 ± 0.1	1.61
threonic acid	2.0 ± 0.2	1.2 ± 0.1	1.64
salicyl alcohol	80.2 ± 5.6	45.3 ± 5.4	1.77
coniferyl alcohol	0.8 ± 0.1	0.5 ± 0	1.77
5-hydroxyferulic acid-glucoside	4.5 ± 0.4	2.4 ± 0	1.84
4-hydroxybenzoic acid	8.7 ± 1.2	4.7 ± 0.2	1.87
palmitic acid	42.3 ± 3.2	22.5 ± 1.4	1.88
syringyl glycerol	1.4 ± 0.2	0.7 ± 0.1	2.14
benzoic acid	2.6 ± 0.3	1.2 ± 0	2.14
ferulic acid	1.0 ± 0.2	0.4 ± 0.1	2.27
dihydroquercetin	0.8 ± 0.1	0.3 ± 0.1	2.28
15.96298312297 salirepin-like	22.9 ± 3.8	9.9 ± 1.8	2.31
succinic acid	11.7 ± 1.7	5.0 ± 0.8	2.33
docosanoic acid	5.0 ± 0.5	2.1 ± 0.1	2.42
14.56171289204	42.2 ± 7.1	16.4 ± 1.8	2.57
17.50259363273 glycoside	43.4 ± 7.6	16.2 ± 1.3	2.68
17.77327259	8.6 ± 1.7	3.2 ± 0.2	2.68
16.55297225 lignan	9.5 ± 1.5	3.4 ± 0.2	2.80
11.74393257303	231.3 ± 25.5	80.0 ± 2.3	2.89
gentisic acid-2-O-glucoside	56.5 ± 11.8	17.6 ± 3.4	3.20
isosalicin	206.8 ± 47.0	57.1 ± 8.2	3.62
17.80259363273 glycoside	287.4 ± 54.9	78.3 ± 11.9	3.67
myo-inositol	344.9 ± 32.1	87.4 ± 0.8	3.94
17.57547457 flavonoid	40.4 ± 8.7	10.2 ± 2.0	3.97
14.25171204217	15.1 ± 2.8	3.6 ± 0.4	4.22
18.13259363273 glycoside	75.5 ± 13.0	17.3 ± 2.5	4.35
17.48547457 flavonoid	51.1 ± 10.1	10.5 ± 1.8	4.89
23.01463219 caffeoyl-shikimate conjugate	1065.8 ± 194.3	130.6 ± 31.8	8.16
22.24 coumaroyl-caffeoyl glycoside	45.6 ± 11.3	4.1 ± 1.1	11.24
20.23171331 coumaroyl conjugate	184.9 ± 52.7	9.6 ± 1.4	19.20

Table 1 (continued)

Metabolite	*PdKOR1* (μg/g FW)	Control (μg/g FW)	Fold change – *PdKOR1*
20.91171 caffeoyl-shikimate conjugate	690.0 ± 115.3	34.1 ± 5.3	20.21
21.17171 caffeoyl shikimate conjugate	351.9 ± 66.9	16.0 ± 2.2	21.95
20.82375597 coumaroyl conjugate	395.0 ± 91.0	15.5 ± 8.3	25.43
20.00171331 coumaroyl conjugate	372.1 ± 66.5	10.8 ± 2.5	34.51
19.72171331 coumaroyl conjugate	240.8 ± 59.3	5.7 ± 0.5	42.55
23.59179 caffeoyl-shikimate conjugate	113.0 ± 19.4	1.7 ± 0.5	66.66
20.68171 caffeoyl conjugate	481.9 ± 88.5	4.3 ± 0.4	112.06
21.66463 caffeoyl glycoside conjugate	50.2 ± 8.5	0	N/A*

Metabolites are organized in ascending order of metabolite fold change in RNAi plants

*denotes a metabolite which was present in RNAi roots and not present in control

rhizospheres and root endospheres, although bacterial and fungal diversity did not differ between *PdKOR1* and controls (Table 2) potentially owing to variation among low replicate numbers.

The Alphaproteobacterial family *Xanthobacteraceae* ($T = -5.81$, $p = 0.01$) and the *Nitrospirae* candidate family *0319-6A21* ($T = -4.50$, $p = 0.02$) had lower abundance in *PdKOR1* RNAi rhizospheres (*Xanthobacteraceae*: 2.0 ± 0.1%; *0319-6A21*: 0.6 ± 0.2%) compared to control rhizospheres (*Xanthobacteraceae*: 2.8 ± 0.1%; *0319-6A21*: 1.8 ± 0.2%). In rhizospheres, the ascomycete order *Pezizales* had greater abundance in *PdKOR1* (1.8 ± 0.1%; $T = 6.07$, $p = 0.01$) versus controls (0.9 ± 0.1%). In root endospheres, the family *Micromonosporaceae* in *Actinobacteria* was greater in *PdKOR1* RNAi (56.7 ± 5.9%) compared to controls (16.1 ± 3.9%; $T = 5.73$, $p = 0.03$). Likewise, the genus *Actinoplanes* in the *Micromonosporaceae*, was more abundant in *PdKOR1* RNAi root endospheres (5.0 ± 1.5%) versus controls (0.1 ± 0.1%). No fungal orders or families in root endospheres differed in abundance between *PdKOR1* and controls ($p \geq 0.14$).

Bacterial and fungal community composition varied across both habitat (bacteria: $R^2 = 0.55$, $p = 0.001$; fungi: $R^2 = 0.31$, $p = 0.001$) and transgenic lines (bacteria: $R^2 = 0.13$, $p = 0.04$; fungi: $R^2 = 0.16$, $p = 0.05$; Fig. 2, Panel A-B). More variation in microbial community composition was explained by habitat effects (rhizophere vs. root endosphere) compared to *PdKOR1* RNAi versus control lines, partially due to greater turnover in OTU frequencies between habitat and the low statistical power of the main effect of transgenics among habitats (*PdKOR1* RNAi plants, $n = 2$; Fig. 2). Both in rhizospheres and root endospheres, there were a large proportion of unique OTUs in vector controls for both bacteria and fungi (not shared with *PdKOR1* RNAi plants). Out of 12,996 and 2706 bacterial OTUs within

Table 2 Summary statistics (mean ± standard error) of microbial diversity estimates and sampling coverage of transgenic lines (*PdKOR1* RNAi, vector control) sampled

Microbial Group	Transgenic Line	Habitat	Goods Coverage	OTU S_{obs}	Simpson's Diversity	Faith's PD	Simpson's Evenness
Bacteria	*PdKOR1* RNAi	Endosphere	0.99 ± 0.002	624 ± 104	0.85 ± 0.01	58 ± 9	0.01 ± 0.002
	PdKOR1 RNAi	Rhizosphere	0.91 ± 0.0002	5386 ± 63	0.99 ± 0.0001	324 ± 1	0.10 ± 0.005
	Control	Endosphere	0.99 ± 0.002	961 ± 247	0.90 ±0.04	84 ± 14	0.01 ± 0.004
	Control	Rhizosphere	0.91 ± 0.001	5525 ± 10	0.99 ±0.0001	329 ± 3	0.09 ± 0.002
Fungi	*PdKOR1* RNAi	Endosphere	0.99 ± 0.0001	42 ± 0	0.69 ± 0.09	n.a.	0.09 ± 0.03
	PdKOR1 RNAi	Rhizosphere	0.97 ± 0.001	553 ± 12	0.93 ± 0.01	n.a.	0.03 ± 0.003
	Control	Endosphere	0.99 ± 0.0003	45 ± 7	0.61 ± 0.11	n.a.	0.06 ± 0.006
	Control	Rhizosphere	0.97 ± 0.002	568 ± 38	0.93 ± 0.03	n.a.	0.03 ± 0.01

S_{obs}, observed OTU richness; Faith's PD, Faith's Phylogenetic Diversity

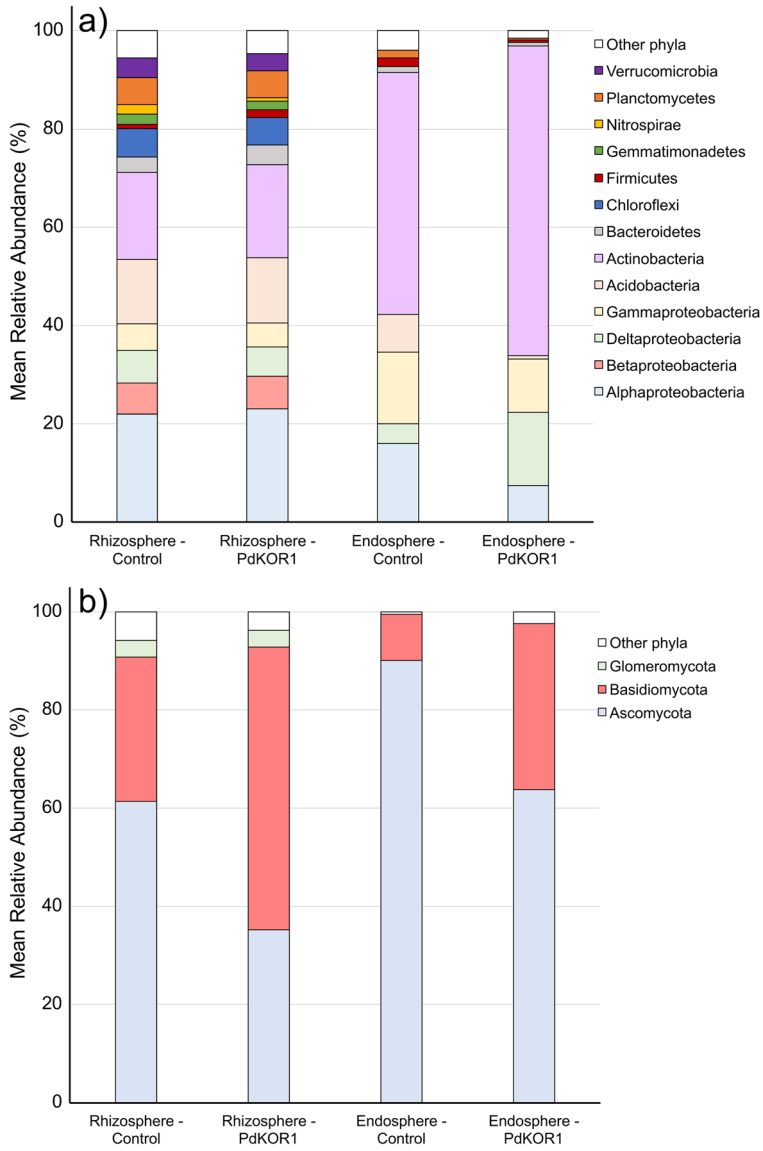

Fig. 1 Mean relative abundance of dominant (≥1.0%) bacterial phyla and subphyla for *Proteobacteria* (Panel **a**) and fungal phyla (Panel **b**) among rhizosphere soils and root endospheres within controls and *PdKOR1* RNAi plants

rhizospheres and root endospheres, respectively, 39% (5081 OTUs) and 63% (1702 OTUs) were unique to vector controls (Fig. 2, Panel C). Out of 1413 and 138 fungal OTUs within rhizospheres and root endospheres, 32% (598 OTUs) and 51% (71 OTUs) were unique to vector controls (Fig. 2, Panel D). Furthermore, 23% (3049 of bacterial OTUs) and 18% (475 of bacterial OTUs) were unique to *PdKOR1* RNAi rhizospheres and root endospheres whereas 24% (335 fungal OTUs) and 28% (39 OTUs) were unique to *PdKOR1* RNAi rhizospheres and root endospheres for fungi, respectively (Fig. 2, Panel C-D).

Pantoea sp. YR343 colonization of PdKOR1

We performed controlled colonization studies using a well-characterized, known *Populus* root colonizer, *Pantoea* sp. sp. YR343, isolated previously from distinct study of *Populus* (Bible et al. 2016; Estenson et al. 2018). In our study, we found the colonization efficacy of *Pantoea* sp. YR343 was significantly reduced in *PdKOR1* RNAi roots compared to the control line ($p = 0.007$; Fig. 3). This suggests that *PdKOR1* gene downregulation and resulting phenotypic changes negatively impacted *Pantoea* colonization of *Populus* roots.

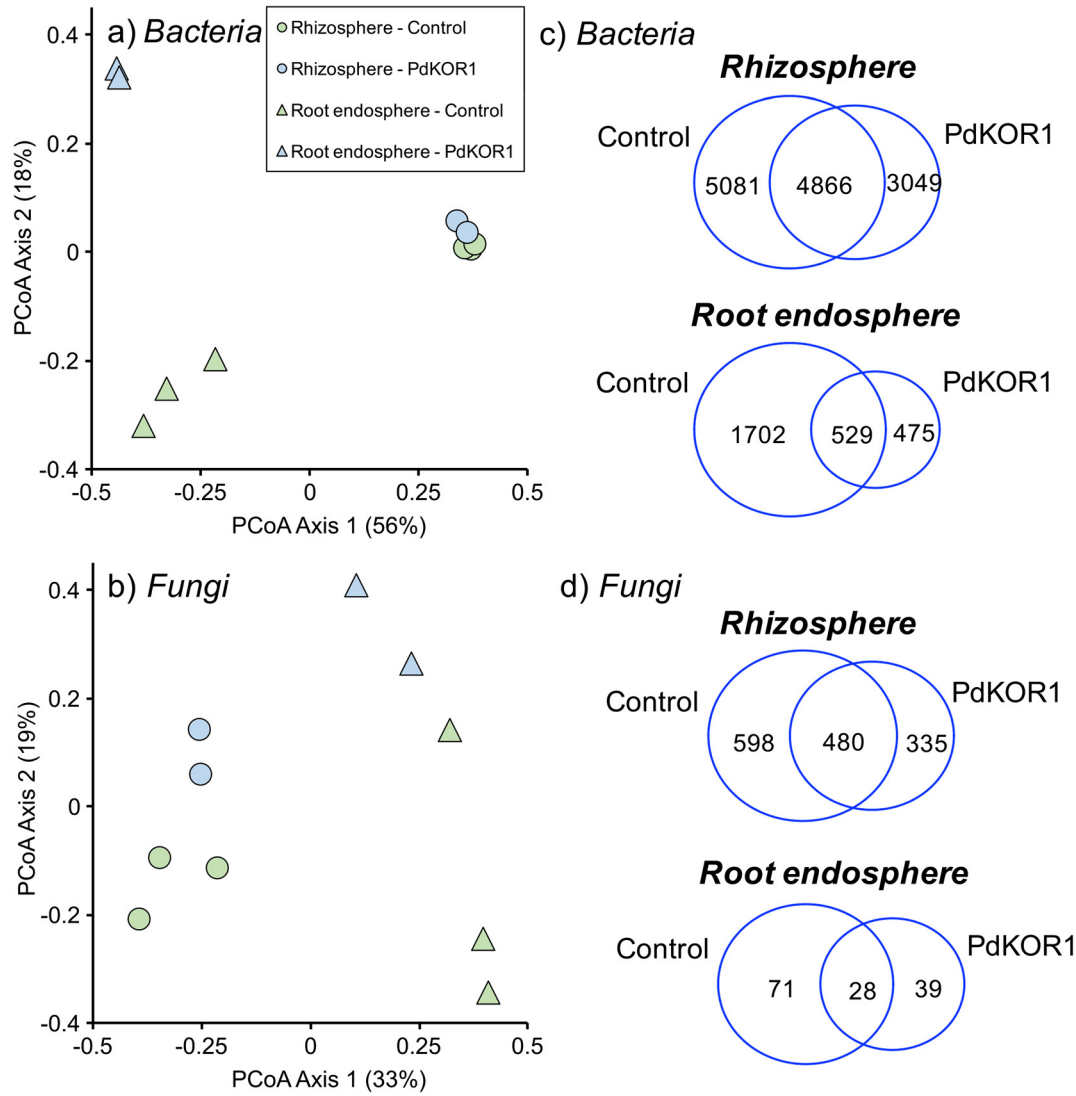

Fig. 2 Principal coordinates analysis (PCoA) of 16S rRNA-based archaeal/bacterial (Panel **a**) and ITS2 rRNA-based fungal (Panel **b**) community composition within rhizosphere and root endosphere habitats in vector control and *PdKOR1* RNAi plants. Venn diagrams are given displaying unique and shared OTUs across rhizosphere and root endosphere habitats in control and RNAi plants for bacteria (Panel **c**) and fungi (Panel **d**). Circle size in panels c-d is scaled based on OTU number within control or RNAi plants in a plant compartment but are not scaled for comparison across rhizosphere and endospheres. Numbers in circles, or in overlapping sections, represent the number of OTUs in that category

Discussion

Down-regulation of *PdKOR1* was found to result in a specific caffeic acid, salicylic acid, and flavonoid metabolite phenotype in field grown roots, similar to effects previously observed in the aboveground tissues of greenhouse-grown plants (Kalluri et al. 2016). Additionally, colonization and assembly of both rhizosphere and root-associated bacterial and fungal communities were divergent in *PdKOR1* RNAi plants from the control plants, indicating plant-microbial interactions are strongly linked to either changes in cell wall chemistry or indirect changes to host physiology and the metabolome. While further studies will be required to parse these possible mechanisms, these results form one of the first studies to address how the root and rhizosphere microbiome is structured in a bioenergy relevant tree species, *Populus deltoides*, which have undergone downregulation of an essential plant cellulose biosynthesis and wall remodeling enzyme.

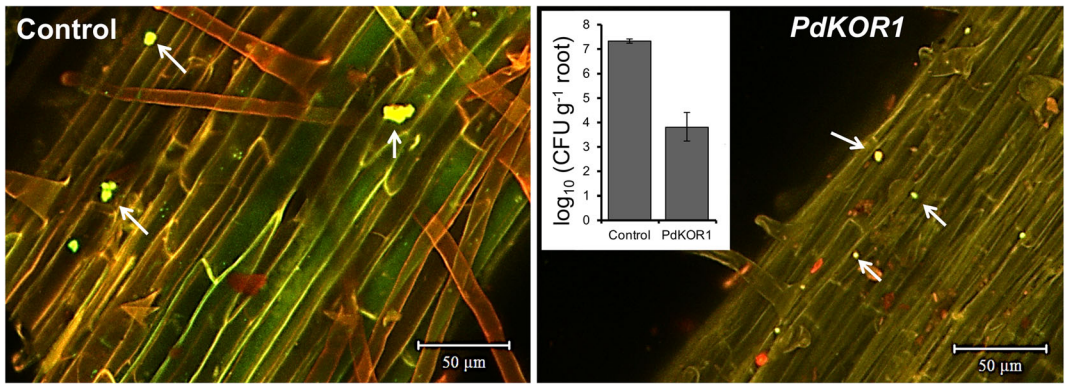

Fig. 3 Confocal imaging of root colonization in *Populus deltoides* control and *PdKOR1* with *Pantoea* YR343-GFP. Colonization of control appears in the form of small aggregates, typical of YR343, whereas *PdKOR1* colonization has individual cells present. Arrows indicate *Pantoea* YR343-GFP attached to the root surface. Colonization of *Populus deltoides* control and *PdKOR1* RNAi plants with *Pantoea* YR343-GFP showed a decrease in root colonization (measured as CFUs per gram of root) in RNAi lines as compared to the control lines ($p = 0.007$)

Aboveground *PdKOR1* RNAi tissue (stems, leaves) have shown to be enriched in salicylic acid-related metabolites (Kalluri et al. 2016). Our study showed that belowground, like aboveground tissues, have increased production of these metabolites (salicyl alcohol and isosalicin). Furthermore, phenolics such as caffeic acid derivatives (i.e., caffeoyl shikimate and its glycoside conjugates) also are enriched in RNAi plants in below- (Table 1) and aboveground (Kalluri et al. 2016) tissue types. These results suggest that both aboveground and belowground secondary carbon metabolism is altered in *PdKOR1* RNAi plants potentially as a result of cellulose and lignin modification in cell walls, and the diversion of lignin synthesis to caffeic and salicylic acid pathways. Contrary to previous work for aboveground *PdKOR1* RNAi plants, free amino acids, such as valine, alanine, and isoleucine, were at a lower level in RNAi roots, whereas other metabolites, such as flavonoids, exhibited increases in RNAi roots compared to controls (Table 1). An altered plant metabolome phenotype of caffeoyl-shikimate and other caffeoyl derivatives (Tschaplinski et al. 2014), salicylic acid-related metabolites (Kalluri et al. 2016), and lignin (Beckers et al. 2016) have been shown to be important factors relevant for microbial colonization and plant – microbe interactions. Furthermore, flavonoids produced by plant roots can act as antimicrobial compounds (Bais et al. 2006) or as species-specific signaling molecules in host plants (Balachandar et al. 2006), and thus possibly linked to inhibition and shifts in microbial colonization patterns. Thus, downregulation of *PdKOR1* and the shifts in secondary C metabolome may partially drive microbial community structure within plant roots.

Downregulation of *PdKOR1* was shown to not only reduce cellulose and lignin content in tissue (Kalluri et al. 2016; Nicol et al. 1998), but also result in reduced growth and cell wall elongation (Zuo et al. 2000). These responses may not only confer disadvantages to plant physiology but may also impact the functional groups and number of microorganisms capable of root endosphere, rhizoplane and rhizosphere colonization. Siciliano and Germida (1999) found that transgenic cultivars of canola (*Brassica napus*) developed to tolerate the herbicide glyphosate (Round-up) had lower bacterial root endophyte diversity, potentially due to the disruption of the chemical (balanced metabolite, nutrient and pH) environment roots provide which select for specific microbial species. In this initial study of field-grown plants, rhizosphere soils had a lower relative abundance of *Nitrospirae* and *Ascomycota* in RNAi plant rhizospheres whereas *Basidiomycota* had a greater relative abundance (Fig. 2). Rhizosphere microbial communities are a subset of bulk soil and can be impacted indirectly by plant root exudates, photosynthates, and plant-microbe signaling (De-la-Peña and Loyola-Vargas 2014). We hypothesize that properties emergent from modified cell wall composition, and carbon partitioning into primary and secondary metabolite pools such as potential changes to metabolism and physiology of the root including root exudate and mucilage composition, and endosphere-specific microbial activity are likely driving the changes observed in dominant microbial group abundances within RNAi plant roots. It is also plausible that the alterations in cell wall biosynthesis translate to reduced cell growth as total root biomass production was reduced relative to

control in RNAi plants (Kalluri et al. 2016). Using microfluidic devices, others have found that in *Arabidopsis thaliana*, *Bacillus subtilis* exhibits chemotaxis towards the elongation zone and excludes *Escherichia coli* from roots (Massalha et al. 2017). Thus, an altered elongation zone physiology can impact root microbial colonization.

RNAi root endospheres exhibited differences in OTU community composition (Fig. 2) and in some microbial phyla, fungal order, and bacterial family-level abundances (Fig. 2). In addition, a large proportion (63%, 51%) of bacterial and fungal OTUs in control root endospheres were unique and did not occur in RNAi plant roots (Panel C-D, Fig. 3). Likewise, 18% of bacterial OTUs and 28% of fungal OTUs were only present in RNAi root endospheres. Therefore, community composition differed not only in OTU frequencies, but also in OTU identity within these tissues for both bacteria and fungi. *PdKOR1* RNAi thus selects for a unique consortium of microbial taxa, and appears to result in reductions in potentially endophytic groups commonly observed in *Populus*, such as Alphaproteobacteria and Gammaproteobacteria (Gottel et al. 2011; Fig. 2), and increases in Actinobacteria (Gottel et al. 2011) such as the *Micromonosporaceae*. We found that colonization of *PdKOR1* RNAi transgenic plants by *Pantoea* YR343, a previously known Gammaproteobacterial associate, was significantly reduced (Fig. 3) compared to the control plants as measured both by colony forming units and direct microscopy of GFP fluorescence, thus confirming that downregulation of *PdKOR1* can reduce microbial colonization in rooting zones for specific taxa. The significantly altered metabolome of *PdKOR1* RNAi plant phenotype may thus allow Actinobacterial groups, like *Micromonosporaceae*, and basidiomycetes to more easily colonize root tissue. Further research addressing linkages among RNAi root architecture, biochemistry, the plant transcriptome, exudate composition and the root endophytic microbiome using constructed community experiments with field-derived isolates is needed to clarify the mechanisms involved in the observed microbial community changes between *PdKOR1* RNAi and control roots.

In conclusion, our study identified the impact of *PdKOR1* gene down-regulation on the root metabolome and microbiome of field-grown *Populus* plants. Modification of host metabolism in *PdKOR1* RNAi background appears to select for unique consortia of microbial taxa. Our study showed reductions in endophytic groups commonly observed in *Populus*, such as Alphaproteobacteria and Gammaproteobacteria and increases in Actinobacteria such as the *Micromonosporaceae*. We also found that colonization of greenhouse-grown *PdKOR1* RNAi transgenic plants by the known poplar root colonizer, *Pantoea* YR343, was significantly reduced (Fig. 3) compared to the control plants as measured both by colony forming units and direct microscopy of GFP fluorescence, thus confirming that downregulation of *PdKOR1* can reduce microbial colonization of host roots for specific taxa. Additional work should address whether the altered root endosphere metabolome translates into an altered exometabolome and whether these changes in the rhizosphere directly impact microbial recruitment in *PdKOR* roots.

These insights from both field and greenhouse conditions demonstrate potential interconnections among plant genotype, cellulose biosynthesis, cell wall properties, host metabolome, and microbial community composition. Specifically, constitutive downregulation of *PdKOR1* and accompanying cell wall modifications result in concomitant changes in host secondary C metabolism and both bacterial and fungal belowground community structure in field-grown *Populus*.

In the future, more expansive efforts to characterize the microbiomes of additional host genotypes contrasted in a suite of cell wall and metabolome changes in the field along with lab and greenhouse-based validation experiments should help clarify whether microbial community differences are a result of metabolomic changes, or due to other phenotypic traits disrupted by *PdKOR1* downregulation. A knowledge base that captures the spectrum of functional implications of biomass chemistry improvement efforts is crucial for meeting the goals of sustainable bioenergy crop production and management.

Acknowledgements We thank Lee Gunter and Meghan Gable for assistance with field work, and Les Pearson and ArborGen Inc. for site maintenance, access and tree harvest permission. We thank Mindy Clark for maintenance of *Populus* plants in the greenhouse. We thank Dr. Jessy Labbe for his comments on a draft of the manuscript. This was research was sponsored by the Genomic Science Program, U.S. Department of Energy, Office of Science, Biological and Environmental Research, as part of the Plant Microbe Interfaces Scientific Focus Area at Oak Ridge National Laboratory (http://www.pmi.ornl.gov). The transgenic plant resource and the Bellville field site maintenance is funded by the BioEnergy Science Center project. The BioEnergy Science Center is a U.S. Department of Energy Bioenergy Research Center supported by the Office of Biological and Environmental Research in the U.S. Department of Energy Office of Science. Oak Ridge National Laboratory is managed by UT-Battelle, LLC, for the U.S. Department of Energy under contract DEAC05-00OR22725.

References

Abarenkov K, Nilsson RH, Larsson KH, Alexander IJ, Eberhardt U, Erland S, Høland K, Kjøller R, Larsson E, Pennanen T, Sen R, Taylor AFS, Tedersoo L, Ursing BM, Vrålstad T, Liimatainen K, Peintner U, Kõljalg U (2010) The UNITE database for molecular identification of fungi – recent updates and future perspectives. New Phytol 186:281–285

Bais HP, Weir TL, Perry LG, Gilroy S, Vivanco JM (2006) The role of root exudates in rhizosphere interactions with plants and other organisms. Annu Rev Plant Biol 57:233–266

Balachandar D, Sandhiya GS, Sugitha TCK, Kumar K (2006) Flavonoids and growth hormones influence endophytic colonization and in plants nitrogen fixation by a diazotrophic *Serratia sp* in rice. World J Microbiol Biotechnol 22:707–712

Bali G, Khunsupat R, Akinosho H, Payyavula RS, Samuel R, Tuskan GA, Kalluri UC, Ragauskas AJ (2016) Characterization of cellulose synthesis of *Populus* plants modified in candidate cellulose biosynthesis genes. Biomass Bioenergy 94:146–154

Baxter HL, Stewart CN Jr (2013) Effects of altered lignin biosynthesis on phenylpropanoid metabolism and plant stress. Biofuels 4:635–650

Beckers B, Op De Beeck M, Weyens N, Van Acker R, Van Montagu M, Boerjan W, Vangronsveld J (2016) Lignin engineering in field-grown poplar trees affects the endosphere bacterial microbiome. Proc Natl Acad Sci U S A 113:2312–2317

Bible AN, Fletcher S, Pelletier DA, Schadt CW, Jawdy SS, Weston DJ, Engle NL, Tschaplinski T, Masyuko R, Polisetti S, Bohn PW, Coutinho TA, Doktycz MJ, Morrell-Falvey JL (2016) A carotenoid-deficient mutant in *Pantoea* sp. YR343, a bacteria isolated from the rhizosphere of *Populus deltoides*, is defective in root colonization. Front Microbiol 7:491. https://doi.org/10.3389/fmicb.2016.00491

Caporaso JG, Kuczynski J, Stombaugh J, Bittinger K, Bushman FD, Costello EK, Fierer N, Gonzalez Peña A, Goodrich JK, Gordon JI, Huttley GA, Kelley ST, Knights D, Koenig JE, Ley RE, Lozupone CA, McDonald D, Muegge BD, Pirrung M, Reeder J, Sevinsky JR, Turnbaugh PJ, Walters WA, Widmann J, Yatsunenko T, Zaneveld J, Knight R (2010) QIIME allows analysis of high-throughput community sequencing data. Nat Methods 7:335–336

Cregger MA, Veach AM, Yang ZK, Crouch MJ, Vilgalys R, Tuskan GA, Schadt CW (2018) The *Populus* holobiont: dissecting the effects of plant niches and genotype on the microbiome. Microbiome 6:31. https://doi.org/10.1186/s40168-018-0413-8

Darley CP, Forrester AM, McQueen-Mason SJ (2001) The molecular basis of plant cell wall extension. Plant Mol Biol 47:179–195

De-la-Peña C, Loyola-Vargas VM (2014) Biotic interactions in the rhizosphere: a diverse cooperative enterprise for plant productivity. Plant Physiol 166:701–719

Edgar RC, Haas BJ, Clemente JC, Quince C, Knight R (2011) UCHIME improves sensitivity and speed of chimera detection. Bioinformatics 15:2194–2200

Estenson K, Hurst GB, Standaert RF, Bible AN, Garcia D, Chourey K, Doktycz MJ, Morrell-Falvey JL (2018) Characterization of Indole-3-acetic acid biosynthesis and the effects of this phytohormone on the proteome of the plant-associated microbe Pantoea sp. YR343. J Proteome Res 17:1361–1374

Fu C, Mielenz JR, Xiao X, Ge Y, Hamilton CY, Rodriguez M Jr, Chen F, Foston M, Ragauskas A, Bouton J, Dixon RA, Wang ZY (2011) Genetic manipulation of lignin reduces recalcitrance and improves ethanol production from switchgrass. Proc Natl Acad Sci U S A 108:3803–3808

Furtado A, Lupoi JS, Hoang NV, Healey A, Singh S, Simmons BA, Henry RJ (2014) Modifying plants for biofuel and biomaterial production. Plant Biotechnol J 12:1246–1258

Gottel NR, Castro HF, Kerley M, Yang Z, Pelletier DA, Podar M, Karpinets T, Uberbacher E, Tuskan GA, Vilgalys R, Doktycz MJ, Schadt CW (2011) Distinct microbial communities within the endosphere and rhizosphere of *Populus deltoides* roots across contrasting soil types. Appl Environ Microbiol 77:5934–5944

Hernández-Blanco C, Feng DX, Hu J, Sánchez-Vallet A, Deslandes L, Llorente F, Berrocol- Lobo M, Keller H, Barlet X, Sánchez-Rodríguez C, Anderson LK, Somerville S, Marco Y, Molina A (2007) Impairment of cellulose synthases required for *Arabidopsis* secondary cell wall formation enhances disease resistance. Plant Cell 19:890–903

Joshi CP, Mansfield SD (2007) The cellulose paradox – simple molecule, complex biosynthesis. Curr Opin Plant Biol 10:220–226

Kalluri UC, Yin H, Yang X, Davison BH (2014) Systems and synthetic biology approaches to alter plant cell walls and reduce biomass recalcitrance. Plant Biotechnol J 12:1207–1216

Kalluri UC, Payyavula RS, Labbé JL, Engle N, Bali G, Jawdy SS, Sykes RW, Davis M, Ragauskas A, Tuskan GA, Tschaplinski TJ (2016) Down-regulation of KORRIGAN-like endo-beta-1,4-glucanase genes impacts carbon partitioning, mycorrhizal colonization, and biomass production in *Populus*. Front Plant Sci 7:1455. https://doi.org/10.3389/fplas.2016.01455

Li M, Pu Y, Ragauskas AJ (2016) Current understanding of the correlation of lignin structure with biomass recalcitrance. Front Chem 4:45. https://doi.org/10.3389/fchem.2016.00045

Liang YK, Xie X, Lindsay SE, Wang YB, Masle J, Williamson L, Leyser O, Hetherington AM (2010) Cell wall composition contributes to the control of transpiration efficiency in *Arabidopsis thaliana*. Plant J 64:679–686

Loqué D, Scheller HV, Pauly M (2015) Engineering of plant cell walls for enhanced biofuel production. Curr Opin Plant Biol 25:151–161

Lundberg DS, Yourstone S, Mieczkowski P, Jones CD, Dangl JL (2013) Practical innovations for high-throughput amplicon sequencing. Nat Methods 10:999–1002

Maloney VJ, Mansfield SD (2010) Characterization and varied expression of a membrane-bound endo-beta-1,4-glucanase in hybrid poplar. Plant Biotechnol J 8:294–307

Martin M (2011) Cutadapt removes adapter sequences from high-throughput sequencing reads. EMBnetjournal 17:10–12

Massalha H, Korenblum E, Malitsky S, Shapiro OH, Aharoni A (2017) Live imaging of root- bacteria interactions in a microfluidics setup. Proc Natl Acad Sci U S A 114:4549–4554

Mendes R, Garvbeva P, Raaijmakers JM (2013) The rhizosphere microbiome: significance of plant beneficial, plant pathogenic, and human pathogenic microorganisms. FEMS Microbiol Rev 37:634–663

Nicol F, His I, Jauneau A, Vernhettes S, Canut H, Hofte H (1998) A plasma membrane-bound putative endo-1,4-beta-D-glucanase is required for normal wall assembly and cell elongation in *Arabidopsis*. EMBIO J 17:5563–5576

Oksanen J, Blanchet FG, Friendly M, Kindt R, Legendre P, McGlinn D, Minchin PR, O'Hara RB, Simpson GL, Solymos P, Stevens MHH, Szoecs E, Wagner H (2017) Package vegan. R package. https://CRAN.R-project.org/package=vegan

Payyavula RS, Tschaplinski TJ, Jawdy SS, Sykes RW, Tuskan GA, Kalluri UC (2014) Metabolic profiling reveals altered sugar and secondary metabolism in response to UGPase overexpression in *Populus*. BMC Plant Biol 14:265

Petersen PD, Lau J, Ebert B, Yang F, Verhertbruggen Y, Kim JS, Varanasi P, Suttangkakul A, Auer M, Loqué D, Scheller HV (2012) Engineering of plants with improved properties as biofuels feedstocks by vessel-specific complementation of xylan biosynthesis mutants. Biotechnol Biofuels 5:84. https://doi.org/10.1186/1754-6834-5-84

Quast C, Pruesse E, Yilmaz P, Gerken J, Schweer T, Yarza P, Peplies J, Glöckner FO (2013) The SILVA ribosomal RNA gene database project: improved data processing and web-based tools. Nucleic Acids Res 41:590–596

R Core Team (2016) R: a language and environment for statistical computing. R Foundation for Statistical Computing, Vienna

Roberts H (2016) Labdsv: ordination and multivariate analysis for ecology. R package. https://ecology.msu.montana.edu/labdsv/R

Shakya M, Gottel N, Castro H, Yang ZK, Gunter L, Labbé J, Muchero W, Bonito G, Vilgalys R, Tuskan G, Podar M, Schadt CW (2013) A multifactor analysis of fungal and bacterial community structure in the root microbiome of mature *Populus deltoides* trees. PLoS One 8:e76382

Siciliano SD, Germida JJ (1999) Taxonomic diversity of bacteria associated with the roots of field-grown transgenic *Brassica napus* cv. *Quest*, compared to the non-transgenic *B. napus* cv. *Excel* and *B. rapa* cv. *Parkland*. FEMS Microbiol Ecol 29: 263–272

Siciliano SD, Fortin N, Mihoc A, Wisse G, Labelle S, Beaumier D, Ouellette D, Roy R, Whyte LG, Banks MK, Schwab P, Lee K, Greer CW (2001) Selection of specific endophytic bacterial genotypes by plants in response to soil contamination. Appl Environ Microbiol 67:2469–2475

Thijs S, Sillen W, Rineau F, Weyens N, Vangronsveld J (2016) Towards an enhanced understanding of plant-microbiome interactions to improve phytoremediation: engineering the metaorganism. Front Microbiol 7:341. https://doi.org/10.3389/fmicb.2016.00341

Thomas LH, Forsyth VT, Sturcová A, Kennedy CJ, May RP, Altaner CM, Apperley DC, Wess TJ, Jarvis MC (2013) Structure of cellulose microfibrils in primary cell walls from collenchyma. Plant Physiol 161:465–476

Tschaplinski TJ, Plett JM, Engle NL, Deveau A, Cushman KC, Martin MZ, Doktycz MJ, Tuskan GA, Brun A, Kohler A, Martin F (2014) *Populus trichocarpa* and *Populus deltoides* exhibit difference metabolomics responses to colonization by the symbiotic fungus *Laccaria bicolor*. Mol Plant Microbe Interact 27:546–556

Urbanowicz BR, Bennet AB, Del Campillo E, Catalá C, Hayashi T, Henrissat B, Höfte H, McQueen-Mason SJ, Patterson SE, Shoseyov O, Teeri TT, Rose JK (2007) Structural organization and a standardized nomenclature for plant endo-1,4-beta-glucanases (cellulases) of glycosyl hydrolase family 9. Plant Physiol 144:1693–1696

Vain T, Crowell EF, Timpano H, Biot E, Desprez T, Mansoori N, Tindade LM, Pagant S, Robert S, Höfte H, Gonneau M, Vernhettes S (2014) The cellulose KORRIGAN is part of the cellulose synthase complex. Plant Physiol 165: 1521–1532

Wang Q, Garrity GM, Tiedje JM, Cole JR (2007) Naïve Bayesian classifier for rapid assignment of rRNA sequences into the new bacterial taxonomy. Appl Environ Microbiol 73: 5261–5267

Yang F, Mitra P, Zhang L, Prak L, Verhertbruggen Y, Kim JS, Sun L, Zheng K, Tang K, Auer M, Scheller HV, Loqué D (2013) Engineering secondary cell wall deposition in plants. Plant Biotechnol J 11:325–335

Zhao Q, Dixon RA (2014) Altering the cell wall and its impact on plant disease: from forage to bioenergy. Annu Rev Phytopathol 52:69–91

Zuo J, Niu Q, Nishizawa N, Wu Y, Kost B, Chua N (2000) KORRIGAN, an *Arabidopsis* endo-1,4-beta-glucanase, localizes to the cell plate by polarized targeting and is essential for cytokinesis. Plant Cell 12:1137–1152